Impact of rice *GENERAL REGULATORY FACTOR14h* (*GF14h*) on low-temperature seed germination and its application to breeding

Yusaku Sugimura[1], Kaori Oikawa[1], Yu Sugihara[2,¤a], Hiroe Utsushi[1], Eiko Kanzaki[1], Kazue Ito[1], Yumiko Ogasawara[1], Tomoaki Fujioka[3], Hiroki Takagi[1,¤b], Motoki Shimizu[1], Hiroyuki Shimono[4,5], Ryohei Terauchi[1,2], Akira Abe[1*]

[1] Iwate Biotechnology Research Center, Kitakami, Iwate, Japan
[2] Crop Evolution Laboratory, Kyoto University, Muko, Kyoto, Japan
[3] Iwate Agricultural Research Center, Kitakami, Iwate, Japan
[4] Faculty of Agriculture, Iwate University, Morioka, Iwate, Japan
[5] Agri-Innovation Center, Iwate University, Morioka, Iwate, Japan

[¤a] Current address: The Sainsbury Laboratory, University of East Anglia, Norwich, United Kingdom
[¤b] Current address: Faculty of Bioresources and Environmental Science, Ishikawa Prefectural University, 1-308, Suematsu, Nonoichi, Ishikawa, 921-8836, Japan

* Corresponding author
E-mail: a-abe@ibrc.or.jp (AA)

ORCIDs
Yusaku Sugimura, 0000-0001-7271-7703
Yu Sugihara, 0000-0001-6042-1091
Hiroki Takagi, 0000-0002-8576-9892
Motoki Shimizu, 0000-0002-5622-5554
Hiroyuki Shimono, 0000-0002-7328-0483
Ryohei Terauchi, 0000-0002-0095-4651
Akira Abe, 0000-0002-0344-2643

Summary

• Direct seeding is employed to circumvent the labor-intensive process of rice (*Oryza sativa*) transplantation, but this approach requires varieties with vigorous low-temperature germination (LTG) when sown in cold climates.

• To investigate the genetic basis of LTG, we identified the quantitative trait locus (QTL) *qLTG11* from high-LTG rice variety Arroz da Terra using QTL-seq.

• We delineated the candidate region to a 52-kb interval containing *GENERAL REGULATORY FACTOR14h* (*GF14h*) gene, which is expressed during seed germination. The Arroz da Terra *GF14h* allele encodes functional GF14h, whereas Japanese rice variety Hitomebore harbors a 4-bp deletion in the coding region. Knocking out functional *GF14h* in a near-isogenic line (NIL) carrying the Arroz da Terra allele decreased LTG, whereas overexpressing functional *GF14h* in Hitomebore increased LTG, indicating that *GF14h* is the causal gene behind *qLTG11*. Analysis of numerous Japanese rice accessions revealed that the functional *GF14h* allele was lost from popular varieties during modern breeding. We generated a NIL in the Hitomebore background carrying a 172-kb genomic fragment from Arroz da Terra including *GF14h*. The NIL showed superior LTG compared to Hitomebore, with otherwise comparable agronomic traits.

• The functional *GF14h* allele from Arroz da Terra represents a valuable resource for direct seeding in cold regions.

Key words

low-temperature seed germination, *GF14h*, *Oryza sativa*, cultivar, genetics, breeding, near-isogenic line, direct seeding

Introduction

Low-temperature seed germination (LTG) is a pivotal agronomic trait in rice (*Oryza sativa*). As rice originated from tropical and subtropical regions, it is highly susceptible to low-temperature conditions compared to other cereal crops such as wheat (*Triticum aestivum*) and barley (*Hordeum vulgare*) (Okuno, 2004). Nevertheless, rice is produced in temperate and high-altitude regions, where it frequently experiences temperatures

below 20°C. In Japan, rice is abundantly cultivated in relatively cold areas such as Tohoku and Hokkaido. In recent years, there has been an increasing demand to shift from conventional transplantation-based rice cultivation to direct seeding to reduce labor and costs. However, direct seeding raises the risk of exposure to low temperatures during seed germination (Iwata *et al.*, 2010). Therefore, to expand the use of direct seeding, it is crucial to breed rice cultivars with enhanced LTG.

LTG is a quantitative trait regulated by complex molecular mechanisms. Linkage mapping and genome-wide association studies (GWAS) have identified over 30 LTG-related quantitative trait loci (QTLs) or genomic regions associated with this trait, located on all 12 rice chromosomes (Miura *et al.*, 2001; Fujino *et al.*, 2004; Han *et al.*, 2006; Jiang *et al.*, 2006; Fujino *et al.*, 2008; Nguyen *et al.*, 2012; Li *et al.*, 2013; Fujino *et al.*, 2015; Pan *et al.*, 2015; Satoh *et al.*, 2015; Jiang *et al.*, 2017; Shakiba *et al.*, 2017; Wang *et al.*, 2018; Jiang *et al.*, 2020; Shim *et al.*, 2020; Yang *et al.*, 2020; Pan *et al.*, 2021; Mao *et al.*, 2022). However, only a few genes involved in LTG have been described, such as *qLTG3-1* (Fujino *et al.*, 2008) and *STRESS-ASSOCIATED PROTEIN16* (*OsSAP16*) (Wang *et al.*, 2018). The *qLTG3-1* gene, encoding a protein of unknown function, has a substantial influence on LTG (Fujino *et al.*, 2008). During seed germination, *qLTG3-1* expression is strongly induced in embryos, which leads to the loosening of the tissues covering the embryo by promoting vacuolation (Fujino *et al.*, 2008). *OsSAP16* encodes a stress-associated protein with two AN1-C2H2 zinc finger domains (Wang *et al.*, 2018). OsSAP16 presumably acts as a regulator of LTG.

14-3-3 proteins are regulatory proteins that are widely conserved in eukaryotes. These proteins bind to phosphorylated serine and tyrosine residues in their target proteins that participate in signal transduction and the regulation of gene expression (Morrison, 2009; Madeira *et al.*, 2015), thus altering their enzymatic activity, subcellular localization, stability, or protein–protein interactions (Hermeking, 2003; Wilson *et al.*, 2016; Camoni *et al.*, 2018). The rice genome encodes eight 14-3-3 proteins, named GF14a–h for GENERAL REGULATORY FACTOR14 (Chen *et al.*, 2006). *GF14h* is involved in rice seed germination under optimal temperature conditions (Sun *et al.*, 2022; Yoshida *et al.*, 2022). In addition, GF14h contributes to phytohormone signaling, including abscisic acid and gibberellin signaling (Sun *et al.*, 2022; Yoshida *et al.*, 2022). However, it remains

unclear whether *GF14h* promotes seed germination under low-temperature conditions (Yoshida *et al.*, 2022).

QTL pyramiding has been proposed as a breeding concept (Ashikari & Matsuoka, 2006) for bringing together several QTLs (or genes) related to agronomically important traits in the genetic background of locally adapted elite cultivars. In practice, it is essential to generate pre-breeding materials for QTL pyramiding, i.e., near-isogenic lines (NILs) that harbor one or a few genomic segments introgressed from the donor parent into the genome of the recipient parent through a combination of continuous backcrossing and selfing via marker-assisted selection (Zhang *et al.*, 2022). In this study, we determined that *GF14h* is responsible for an LTG-related QTL in Portuguese rice variety Arroz da Terra. We generated a NIL in the background of rice cultivar Hitomebore, which is adapted for growth in northern Japan, by replacing its *GF14h* genomic fragment with that from Arroz da Terra and tested its LTG performance.

Materials and Methods

Plant materials

Rice was cultivated in a paddy field at Iwate Agricultural Research Center (39°35'N, 141°11'E). A recombinant inbred line (RIL) population of 200 F_7 lines was generated from a cross between Japanese variety Iwatekko and the high-LTG variety Arroz da Terra (Fig. S1) (Takagi *et al.*, 2013). To develop NILs, rice cultivar Hitomebore was used as the recipient parent to generate NILs harboring the target genomic region from Arroz da Terra (Fig. S2a), thereby establishing *qLTG3-2*-NIL, *qLTG11*-NIL, and NIL-$GF14h^{Arroz}$ (Figs. 1c, S2b, S3a).

Evaluation of germination rate

Seeds for each line were harvested 45 days after heading, air-dried at 30°C for two days, and stored at 4°C until use. The seeds were air-dried at 50°C for seven days in the dark to break dormancy. For germination tests, 50 seeds per replicate were incubated in a Petri dish filled with distilled water in the dark at 15°C (low-temperature conditions) or 25°C (optimal temperature conditions). The germination rate was calculated as the total number of germinated seeds at each time point divided by the number of seeds tested. Seeds were

125 considered to have germinated when the white coleoptile was visible.

126 To evaluate resistance to pre-harvest sprouting, panicles were harvested from
127 NIL-*GF14h*^{Arroz} and Hitomebore 30 days after heading. The panicles were incubated in
128 dark, wet conditions (by covering them with filter paper moistened with water) at 28°C
129 for 10 days, and seed germination was scored.

130

131 **QTL-seq analysis**

132 LTG data for the 200 RILs derived from a cross between Iwatekko and Arroz da Terra
133 (Fig. S1) were analyzed (Takagi *et al.*, 2013). The top 20 RILs showing high-LTG and
134 the bottom 20 RILs showing low-LTG phenotypes were selected to assemble the two bulk
135 samples with contrasting LTG phenotypes. All seedlings with high or low LTG were
136 pooled, and DNA was extracted from each bulk as previously described (Takagi *et al.*,
137 2013). The genomic DNA of the two bulks was used to generate DNA-seq libraries and
138 sequenced on a GAIIx sequencer (Illumina, CA, USA). QTL-seq was performed to
139 identify QTLs related to LTG (Takagi *et al.*, 2013; Sugihara *et al.*, 2022).

140

141 **Map-based cloning of *qLTG11***

142 To narrow down the *qLTG11* region, genotyping was performed using a cross population
143 of *qLTG11*-NIL (BC_2F_3) backcrossed to Hitomebore. The germination rate under low-
144 temperature conditions (15°C) was measured to characterize LTG activity. High-
145 resolution fine mapping with ten markers (markers B−K) between 23.466 Mb and 23.609
146 Mb on chromosome 11 identified six informative recombinants in the target region.
147 Primers used for mapping are listed in Table S1.

148

149 ***De novo* assembly of the Hitomebore and Arroz da Terra genomes**

150 To reconstruct the *qLTG11* regions in Hitomebore and Arroz da Terra, *de novo* assembly
151 was performed for each genome using Nanopore long reads and Illumina short reads
152 according to a published method (Sugihara *et al.*, 2023). To extract high-molecular-
153 weight genomic DNA from leaf tissue for Nanopore sequencing, a NucleoBond high-
154 molecular-weight DNA kit (MACHEREY-NAGEL, Germany) was used. Following
155 DNA extraction, low-molecular-weight DNA was eliminated using a Short Read

156 Eliminator Kit XL (Circulomics, MD, USA). Library preparation was then performed
157 using a Ligation Sequencing Kit (SQK-LSK-109; Oxford Nanopore Technologies [ONT],
158 United Kingdom) according to the manufacturer's instructions, and sequencing was
159 performed using MinION (ONT, UK) for Arroz da Terra. For Hitomebore, Nanopore long
160 reads sequenced by Sugihara et al. (2023) were used. Base-calling of the Nanopore long
161 reads was performed using Guppy 4.4.2 (ONT, UK). Sequences derived from the lambda
162 phage genome were removed from the raw reads with NanoLyse v1.1.0 (De Coster *et al.*,
163 2018). The first 50 bp of each read were then removed, as were reads with an average
164 read quality score below 7 and reads shorter than 3,000 bases, using NanoFilt v2.7.1 (De
165 Coster *et al.*, 2018). The clean Nanopore long reads were assembled using NECAT v0.0.1
166 (Chen *et al.*, 2021), setting the genome size to 380 Mb. To improve the accuracy of
167 assembly, Racon v1.4.20 (Vaser *et al.*, 2017) was used twice for error correction using
168 Nanopore reads, and Medaka v1.4.1 (https://github.com/nanoporetech/medaka) was
169 subsequently used to correct mis-assembly. Two rounds of consensus correction were
170 then performed using bwa-mem v0.7.17 (Li & Durbin, 2009) and HyPo v1.0.3 (Kundu *et*
171 *al.*, 2019) with the Illumina short reads. Redundant contigs were removed using purge-
172 haplotigs v1.1.1 (Roach *et al.*, 2018), resulting in a *de novo* assembly of 374.8 Mb
173 comprising 82 contigs for Hitomebore and 376.3 Mb consisting of 82 contigs for Arroz
174 da Terra. The resulting genome sequences have been deposited in Zenodo
175 (https://doi.org/10.5281/zenodo.10460309).
176

177 **Plant transformation**

178 To generate *GF14h* knockout mutants, two single guide RNAs (sgRNAs) targeting exon
179 4 or exon 5 of *GF14h* were designed using the web-based service CRISPRdirect
180 (crispr.dbcls.jp) (Naito *et al.*, 2015) and cloned individually into the
181 pZH::OsU6gRNA::MMCas9 vector (Mikami *et al.*, 2015). The resulting vectors were
182 introduced into Agrobacterium (*Agrobacterium tumefaciens*) strain EHA105 for
183 transformation into *qLTG11*-NIL plants (Toki *et al.*, 2006). The target sites in the positive
184 transformants were sequenced by Sanger sequencing to detect mutations. To obtain
185 overexpression constructs, the full-length coding sequence of functional *GF14h* was
186 amplified from total RNA extracted from *qLTG11*-NIL and cloned into the plant binary

187 vector pCAMBIA1300 under the control of the cauliflower mosaic virus (CaMV) 35S
188 promoter. The overexpression plasmid was introduced into Agrobacterium strain
189 EHA105 for transformation of rice variety Hitomebore (Toki *et al.*, 2006). All primers
190 used are listed in Table S1.
191

192 **Expression analysis**

193 Total RNA was extracted from germinating seeds using an RNA-suisui S kit (Rizo). Total
194 RNA was treated with RNase-free DNase I (Nippon Gene). The resulting samples were
195 reverse transcribed into first-strand cDNA using a PrimeScript RT Reagent Kit (Takara
196 Bio). Quantitative PCR (qPCR) was conducted using a QuantStudio 3 system (Thermo
197 Fisher Scientific) with Luna Universal qPCR Master Mix (New England Biolabs). The
198 cycling parameters were 1 min at 95°C, followed by 40 cycles of amplification (95°C for
199 15 sec and 60°C for 30 sec). The *Actin* gene (Os03g0718100) served as an internal control,
200 and the Delta CT method was used to calculate the relative expression levels. The primer
201 sets are listed in Table S1.
202

203 **RNA-seq**

204 Total RNA was extracted from Hitomebore and *qLTG11*-NIL seeds at 0, 1, 2, and 3 days
205 after the onset of seed hydration under low (15°C) or optimum (25°C) temperature
206 conditions using an RNA-suisui S kit (Rizo, Ibaraki, Japan). Sequencing libraries were
207 prepared using an NEBNext Ultra II Directional RNA Library Prep Kit for Illumina (New
208 England Biolabs Japan, Tokyo, Japan) following the manufacturer's protocol. The
209 libraries were sequenced in paired-end mode using an Illumina HiSeq X instrument
210 (Illumina, CA, USA). The raw reads have been deposited in the DNA Databank of Japan
211 (BioProject accession No. PRJDB17450). For quality control, reads shorter than 50 bases
212 and those with an average read quality below 20 were discarded using Trimmomatic v0.36
213 (Bolger *et al.*, 2014), and poly(A) sequences were trimmed using PRINSEQ++ v1.2
214 (Cantu *et al.*, 2019). The resulting clean reads were aligned to the *de novo* assembled
215 Hitomebore and Arroz da Terra genomes with HISAT2 v2.1 (Kim *et al.*, 2019). BAM
216 files were sorted and indexed with SAMtools v1.10 (Li *et al.*, 2009), and aligned reads
217 were assembled into transcripts with StringTie (Pertea *et al.*, 2015) by combining bam

218 files for each variety.

219

220 Haplotype network analysis

221 Sequencing datasets were obtained for 503 rice accessions. Of these, 379 were FASTQ
222 files downloaded from the DNA Data Bank of Japan Sequence Read Archive (DRA)
223 (Yabe *et al.*, 2018; Tanaka *et al.*, 2020; Tanaka *et al.*, 2021; Shimono *et al.*, 2023) and
224 124 were sequenced in this study (Table S2). Details about DNA extraction, whole-
225 genome sequencing techniques, and construction of the genotype datasets in VCF format
226 are provided in a previous report (Shimono *et al.*, 2023). This study specifically focused
227 on the coding region of *GF14h*. Genotype information related to the coding region of
228 *GF14h* was extracted from the VCF dataset. In addition, the *k*-mer analysis program
229 (https://github.com/taitoh1970/kmer) (Itoh *et al.*, 2020) was used with Illumina short
230 reads to detect the 4-bp deletion with high sensitivity. Genotype information for the
231 presence of the 4-bp deletion was added to the VCF file, and 81 samples with
232 heterozygous genotypes were discarded. A haplotype network was then constructed using
233 the median-joining network algorithm (Bandelt *et al.*, 1999) implemented in Popart v1.7
234 (Leigh *et al.*, 2015).

235

236 Evaluation of agronomic traits and yield performance of NIL-
237 *GF14h*^{Arroz}

238 The grain yields of Hitomebore and NIL-*GF14h*^{Arroz} were investigated in experimental
239 paddy fields in 2023. Field experiments were conducted at the Iwate Agricultural
240 Research Center (39°35'N, 141°11'E) in Kitakami, Iwate, Japan. A fertilization regime of
241 $N:P_2O_5:K_2O$ = 6:6:6 g m^{-2} was applied as a basal dressing, and $N:K_2O$ = 2:2 g m^{-2} was
242 applied as a top dressing. Seeds were sown in a seedling nursery box on 21 April, and
243 seedlings were transplanted to the paddy field on 18 May. To evaluate agronomic traits,
244 the seedlings were transplanted at a rate of one plant per hill, with a planting density of
245 22.2 hills m^{-2}. Culm length, panicle length, panicle number, grain number per plant, and
246 grain weight per plant were measured at maturity. To evaluate yield performance,
247 seedlings were transplanted with three plants per hill at a planting density of 16.7 hills
248 m^{-2}. The 0.9 × 5.0 m experimental plots in the paddy fields were arranged in a randomized

complete block design with three replicates. At maturity, 50 hills were harvested from each plot to measure brown rice yield. The hulls were removed using a rice huller (Model 25MC, Ohya Tanzo Factory Co., Ltd., Japan), and the hulled grains were screened with a grain sorter (1.9-mm sieve size). Brown rice yields were adjusted to 15% moisture content and converted to weight per hectare.

Results

Evaluation of QTLs associated with low-temperature germination using the Portuguese rice variety Arroz da Terra

The Portuguese rice variety Arroz da Terra germinates more vigorously under low-temperature conditions than the Japanese cultivars Iwatekko and Hitomebore (Fig. 1a). To identify the genes responsible for this difference, we searched for QTLs involved in the high LTG of Arroz da Terra. We previously generated a set of 200 RILs at the F_7 generation derived from a cross between Arroz da Terra and Iwatekko (Fig. S1) (Takagi *et al.*, 2013). We phenotyped all RILs for LTG and selected the 20 RILs with the highest LTG and the 20 RILs with the lowest LTG. We assembled two pools of seedlings with low or high LTG and extracted their genomic DNA for whole-genome sequencing on the Illumina platform (Fig. S1) (Takagi *et al.*, 2013). We mapped the resulting sequencing reads to the Nipponbare rice reference genome (IRGSP-1.0) and performed QTL-seq analysis using our new high-performance pipeline (Sugihara *et al.*, 2022). Based on the ΔSNP index, we identified three QTLs related to LTG on chromosome 3 (*qLTG3-1* and *qLTG3-2*) and chromosome 11 (*qLTG11*) (Fig. 1b), which is consistent with the results of a previous study (Takagi *et al.*, 2013).

The *qLTG3-1* region contained the gene Os03g0103300, which was reported to be involved in LTG in a study using rice cultivar Italica Livorno, which has high LTG, and Hayamasari, which has low LTG (Fujino *et al.*, 2008). An examination of its coding sequences in Arroz da Terra, as well as Iwatekko and Hitomebore, revealed that they were identical to those found in Italica Livorno and Hayamasari, respectively (Fig. S4). While Italica Livorno harbored a functional haplotype for this gene, Hayamasari carried a loss-of-function haplotype due to a 71-bp deletion (Fig. S4) (Fujino *et al.*, 2008). Therefore, we propose that the causal gene for the QTL *LTG3-1* is Os03g0103300.

280 To evaluate the contribution of the two other QTLs to LTG, we generated NILs
281 harboring a segment from the Arroz da Terra genome for each QTL (approximately 5 Mb)
282 in the Hitomebore background (Figs. 1c, S2a, S3a). We detected no clear effect on LTG,
283 as *qLTG3-2*-NIL and Hitomebore showed similar seed germination rates at 15ºC (Fig.
284 S3b). By contrast, the germinability of *qLTG11*-NIL was more vigorous than that of
285 Hitomebore at 15ºC (Fig. 1d), indicating that *qLTG11* enhances LTG. *qLTG11*-NIL seeds
286 also germinated more rapidly than Hitomebore seeds under normal conditions (25ºC),
287 although with a smaller difference between the two genotypes than at low temperature
288 (Fig. S5). We therefore focused our analysis on *qLTG11*.
289

290 **Identification of *GF14h* as the candidate gene for *qLTG11***

291 To delineate the *qLTG11* region, we carried out map-based cloning using a segregating
292 population derived from a cross between BC_2F_3 line *qLTG11*-NIL and Japanese elite
293 cultivar Hitomebore (Fig. S2a). For mapping, we conducted germination tests at 15°C.
294 We narrowed down the genomic region containing the QTL to a 52-kb segment (from
295 23.512 bp to 23.564 Mb) on chromosome 11 based on the Nipponbare reference genome
296 (IRGSP-1.0) (Fig. 2a). This interval contains two annotated genes based on the
297 Nipponbare genome sequence (Fig. 2b). We compared the genomic sequence of
298 Hitomebore and Arroz da Terra across the candidate region using *de novo* genome
299 assembly obtained from Nanopore long reads. The cultivars Hitomebore and Nipponbare
300 had an identical genomic sequence over the entire candidate region (Fig. S6a). By contrast,
301 the genome sequence from Arroz da Terra was substantially different from that of
302 Nipponbare, with the equivalent candidate region spanning approximately 94 kb (Figs 2b,
303 S6b).
304 As the causal gene behind the variation in LTG is likely expressed in seeds, we
305 performed transcriptome deep sequencing (RNA-seq) during seed germination in
306 Hitomebore and *qLTG11*-NIL. Within the candidate region, the gene Os11g0609600,
307 corresponding to the *14-3-3* gene *GF14h*, was expressed in both Hitomebore and
308 *qLTG11*-NIL. The *GF14h* gene structure and haplotypes in Arroz da Terra and
309 Hitomebore are shown in Fig. 2c. We detected a 4-bp deletion in the *GF14h* coding region
310 in Hitomebore, causing a frameshift mutation predicted to introduce a premature stop

311 codon (Figs. 2c, S7). These results suggest that Hitomebore carries a loss-of-function
312 allele of *GF14h*. To assess the role of *GF14h* in LTG, we examined the expression pattern
313 of the putative functional *GF14h* (*GF14h*^{Arroz}) allele during seed germination at low
314 temperature (15°C) using *qLTG11*-NIL. RT-qPCR analysis of *GF14h* expression levels
315 showed that they were comparable in the embryo and endosperm at 1 and 3 days after the
316 onset of seed imbibition (Fig. 2d). At the beginning of germination, when a white
317 coleoptile was visible (5 and 7 days after seed imbibition), *GF14h* expression levels rose
318 in the endosperm, but not in the embryo (Fig. 2d). By nine days of imbibition, when most
319 seeds had germinated, *GF14h* expression in the endosperm returned to basal levels (Fig.
320 2d). These results support the notion that *GF14h* plays a role in seed germination at low
321 temperature.
322

323 ## *GF14h* plays a vital role in LTG

324 To investigate the contribution of GF14h to LTG, we knocked out the functional *GF14h*
325 copy present in *qLTG11*-NIL by clustered regularly interspersed short palindromic repeat
326 (CRISPR)/CRISPR-associated nuclease 9 (Cas9)-mediated gene editing and evaluated
327 LTG. Specifically, we introduced two single guide RNA (sgRNA) constructs targeting the
328 exons of *GF14h* individually into *qLTG11*-NIL by Agrobacterium-mediated
329 transformation. We chose to knock out *GF14h* in the *qLTG11*-NIL background rather than
330 Arroz da Terra to evaluate the specific contribution of *GF14h* to LTG without the
331 influence of *qLTG3-1*, which would be present in the Arroz da Terra background. To
332 accurately evaluate the phenotypes of the edited plants, we selected heterozygous plants
333 in the T_0 generation and isolated homozygous mutant lines and their unedited
334 homozygous siblings in the T_1 generation. We obtained four knockout lines (*gf14h-1*,
335 *gf14h-2*, *gf14h-3*, and *gf14h-4*) and their wild-type sibling (WT^{Arroz}) (Fig. S8). We
336 detected significant drops in LTG rates in all four knockout lines compared to WT^{Arroz}
337 (Fig. 3a,b). Furthermore, we generated transgenic lines in the Hitomebore background
338 overexpressing the functional *GF14h* allele from Arroz da Terra under the control of the
339 CaMV 35S promoter. In these overexpression lines, *GF14h* expression increased
340 approximately 1,000-fold compared to the wild-type sibling (WT^{Hitomebore}) (Fig. S9).
341 Importantly, the overexpression lines showed higher LTG than WT^{Hitomebore} when tested

342 at 15ºC (Fig. 3c,d). Taken together, these data indicate that *GF14h* is a key gene involved
343 in LTG.
344

345 Loss-of-function alleles *GF14h* and *qLTG3-1* increased in frequency 346 during rice breeding in Japan

347 We reconstructed the *GF14h* haplotype network using genotype data obtained from
348 whole-genome resequencing of 492 *O. sativa* accessions from various collections,
349 including the World Rice Core Collection (Tanaka *et al.*, 2020), the Rice Core Collection
350 of Japanese Landraces (Tanaka *et al.*, 2021), and a set of Japanese landraces and modern
351 varieties (Shimono *et al.*, 2023), in addition to 11 wild rice (*O. rufipogon*) accessions
352 (Zhao *et al.*, 2018) (Table S2). We distinguished 10 haplotypes for the *GF14h* coding
353 region based on 11 polymorphic sites comprising one frameshift mutation caused by a 4-
354 bp deletion, four nonsynonymous single nucleotide polymorphisms (SNPs), and six
355 synonymous SNPs (Table S3). The conversion of the functional allele Hap2 to its
356 nonfunctional allele Hap1 required only a single step: a 4-bp deletion (Fig. S10).
357 We analyzed the haplotype frequencies of *GF14h* and *qLTG3-1* in Japanese
358 landraces and cultivars, which we grouped according to their time of release. More than
359 half of all Japanese landraces carried functional alleles of both *GF14h* and *LTG3-1* (Fig.
360 4a). The next most common allele combination was a nonfunctional *GF14h* allele with a
361 functional *LTG3-1* allele (Fig. 4a). The percentage of lines with loss-of-function alleles
362 at both *GF14h* and *LTG3-1* has increased since the beginning of crossbreeding in Japan
363 in the early 20th century, with more than 80% of varieties released after 2001 carrying
364 loss-of-function alleles for both genes (Fig. 4a,b). Looking at each gene separately in
365 landraces, only a few lines carried a loss-of-function allele for *LTG3-1*, whereas roughly
366 half of all lines already harbored a loss-of-function allele for *GF14h* (Fig. 4b). Modern
367 breeding thus appears to have increased the proportion of loss-of-function alleles for these
368 two genes, with a substantial increase in *LTG3-1*, reaching almost 90% among lines bred
369 after 2001 (Fig. 4b).
370

371 The Arroz da Terra *GF14h* allele could be valuable for rice breeding

372 To assess how useful the above findings might be to practical breeding programs, we

373 developed new breeding materials. QTL pyramiding, a strategy for introducing multiple
374 QTLs for desired traits into a single genetic background, is a key strategy employed in
375 current breeding. An essential step in QTL pyramiding is the generation of NILs
376 containing the desired QTLs. Therefore, we developed a NIL, termed NIL-*GF14h*^{Arroz},
377 using the elite cultivar Hitomebore as the genetic background into which we introgressed
378 a 172-kb region from the Arroz da Terra genome containing *GF14h* (Fig. S2). This NIL
379 showed a higher seed germination rate under low-temperature conditions compared to
380 Hitomebore (Fig. 5a,b). In addition, NIL-*GF14h*^{Arroz} was slightly more susceptible to pre-
381 harvest sprouting than Hitomebore (Fig. S11). Importantly, we observed no substantial
382 differences in five agronomic traits (culm length, panicle length, panicle number, grain
383 number, and grain weight) between NIL-*GF14h*^{Arroz} and Hitomebore (Fig. 5c-g). Brown
384 rice yield was slightly lower in NIL-*GF14h*^{Arroz} compared to Hitomebore, but a sufficient
385 yield was guaranteed (Fig. 5h,i). These results suggest that NIL-*GF14h*^{Arroz} could be a
386 valuable parental line for breeding via QTL pyramiding.
387

388 # Discussion

389 Here, we demonstrated that the functional *GF14h* allele present in Portuguese rice variety
390 Arroz da Terra plays a pivotal role in supporting seed germinability under low-
391 temperature conditions. Although the regulation of seed germination by *GF14h* was
392 recently documented, its activity under low-temperature conditions remained unclear
393 (Sun *et al.*, 2022; Yoshida *et al.*, 2022). While many genomic regions associated with
394 LTG have been detected through QTL mapping and GWAS, only a few studies have
395 identified the causal genes (Miura *et al.*, 2001; Fujino *et al.*, 2004; Han *et al.*, 2006; Jiang
396 *et al.*, 2006; Fujino *et al.*, 2008; Nguyen *et al.*, 2012; Li *et al.*, 2013; Fujino *et al.*, 2015;
397 Pan *et al.*, 2015; Satoh *et al.*, 2015; Jiang *et al.*, 2017; Shakiba *et al.*, 2017; Wang *et al.*,
398 2018; Jiang *et al.*, 2020; Shim *et al.*, 2020; Yang *et al.*, 2020; Pan *et al.*, 2021; Mao *et al.*,
399 2022). Indeed, LTG is a quantitative trait involving the cumulative effects of multiple
400 genes and their epistatic relationships, making it difficult to assess the specific effect of a
401 single genomic region on LTG. To eliminate the influence of other chromosomal regions
402 on LTG, we first generated *qLTG11*-NIL containing only one of three QTLs detected in
403 the Arroz da Terra background for genetic analysis. The analysis of *qLTG11*-NIL revealed

404 that *GF14h* participates in LTG. Significantly, the NIL harboring the functional *GF14h*
405 allele from Arroz da Terra in the Hitomebore background provides valuable pre-breeding
406 materials for QTL pyramiding. These findings provide a genetic understanding of low-
407 temperature germinability as well as new resources for rice breeding.
408

409 **Influence of *GF14h* on low-temperature germination**

410 In this study, we identified *GF14h* as being implicated in LTG. In a previous study, a
411 genetic complementation assay with a functional *GF14h* allele introduced into the rice
412 cultivar Nipponbare background increased the germination rate at 30°C, but only to a
413 limited extent at 15°C (Yoshida *et al.*, 2022). This result is not consistent with our finding
414 that introducing functional *GF14h* into Hitomebore resulted in a significant improvement
415 in germination at low temperature. Perhaps this discrepancy is due to differences in the
416 rice varieties used in the germination assays. Notably, the haplotypes of *qLTG3-1*, a major
417 QTL behind LTG (Fujino *et al.*, 2008), are different between Nipponbare and
418 Hitomebore: whereas Nipponbare, which was released in 1961, harbors the functional
419 allele of *qLTG3-1*, Hitomebore carries a loss-of-function allele with a deletion of 71 bp
420 (Fig. S4) (Hori *et al.*, 2010). Moreover, the cultivars Koshihikari and Hayamasari, which
421 carry the same loss-of-function *qLTG3-1* allele as the Hitomebore variety, were reported
422 to exhibit lower germination rates at low temperatures than Nipponbare (Hori *et al.*, 2010).
423 LTG tests using chromosome segment substitution lines derived from a cross between
424 Koshihikari and Nipponbare indicated that *qLTG3-1* contributes to the difference in LTG
425 between the two varieties (Hori *et al.*, 2010). Based on these observations, it is likely that
426 Nipponbare has a better LTG ability than Hitomebore, which may have masked the effect
427 of functional *GF14h* on LTG in the previous study (Yoshida *et al.*, 2022). Our study
428 confirmed the involvement of *GF14h* in LTG through map-based cloning and analysis of
429 knockout and overexpression lines. It is also worth mentioning that our experiments were
430 performed in the *qLTG11*-NIL background, which allowed us to isolate the contribution
431 of GF14h to LTG without any influence from *qLTG3-1* or other genes in the Arroz da
432 Terra background. In summary, we provided multiple lines of evidence that *GF14h*
433 contributes to LTG.
434 The expression pattern of functional *GF14h* during seed germination was

435 previously unclear. While *GF14h* has been shown to be expressed in the aleurone layer
436 surrounding the embryo (Yoshida *et al.*, 2022), it is also highly expressed in the
437 endosperm (Sun *et al.*, 2022). In the current study, we showed that *GF14h* was expressed
438 throughout the seeds, but with a transient induction in expression in the endosperm at
439 roughly the time of initiation of seed germination. GF14h was reported to regulate seed
440 germination by interacting with the abscisic acid and gibberellin signaling pathways at
441 optimal temperatures (Sun *et al.*, 2022; Yoshida *et al.*, 2022). We therefore suggest that
442 GF14h controls LTG by interacting with various phytohormone signaling pathways.
443

444 Low-temperature germinability in rice was lost due to selection in 445 modern Japanese breeding

446 In this study, we performed haplotype network analysis of *GF14h* using many Japanese
447 rice varieties. We identified ten distinct haplotypes based on 11 polymorphic sites in the
448 *GF14h* coding region. Of these, Hap4, encompassing the aus, indica, tropical japonica,
449 temperate japonica, and *O. rufipogon* accessions, was defined at the center of the
450 haplotype network. Furthermore, we determined that a 4-bp deletion converted the
451 functional haplotype Hap2, which was derived from Hap4, into the nonfunctional
452 haplotype Hap1. This finding is consistent with the relationship between Hap6 and Hap1
453 (which we defined as Hap2 and Hap1, respectively) observed by Sun *et al.* (2022). These
454 results suggest that the nonfunctional allele represented by Hap1 was introduced into
455 temperate *japonica* varieties from tropical *japonica* varieties carrying Hap2 and then
456 spread to Japanese cultivars.
457 We studied the haplotype frequencies of *GF14h* and *qLTG3-1* in various Japanese
458 landraces and cultivars, considering their time of release from breeding programs into the
459 field. More than half of the Japanese landraces analyzed carried both functional *GF14h*
460 and *qLTG3-1* alleles. However, the frequency of varieties carrying loss-of-function alleles
461 for both *GF14h* and *qLTG3-1* has increased since crossbreeding began in the early 20th
462 century. This trend has continued to the present, perhaps as a result of artificial selection
463 to improve resistance to pre-harvest sprouting, with more than 80% of all varieties bred
464 since 2001 carrying these loss-of-function alleles.
465 Our study provides a historical perspective on allelic shifts in Japanese rice breeding

466 while highlighting the influence of modern breeding on genetic diversity. Further research
467 is needed to elucidate the potential effects of higher frequencies of loss-of-function alleles
468 on the overall phenotypic characteristics and ecological adaptability of Japanese rice
469 varieties. In addition, as mentioned in previous reports (Sun *et al.*, 2022; Yoshida *et al.*,
470 2022), we believe that the reintroduction of functional alleles should be considered in
471 order to develop cultivars suitable for labor-saving cultivation techniques such as direct
472 seeding.
473

474 **Application to direct seeding for rice cultivation**

475 Cultivation stability under direct seeding conditions is important for managing rice
476 production costs and reducing labor. However, since rice is sensitive to low temperatures,
477 improving seed germination and seedling establishment at low temperatures is a desirable
478 breeding trait in high-latitude rice production areas such as Japan. In the current study,
479 we developed a potentially useful NIL (NIL-*GF14h*^{Arroz}) by introducing the functional
480 *GF14h* allele into the Hitomebore background. Overexpressing this functional *GF14h*
481 allele was previously shown to improve anaerobic germination and tolerance to seedling
482 establishment under anaerobic conditions in laboratory experiments (Sun *et al.*, 2022).
483 However, whether NIL-*GF14h*^{Arroz} exhibits strong seedling vigor at low temperatures in
484 rice fields remains to be determined. We previously identified a QTL associated with
485 seedling vigor, *qPHS3-2* (QTL for plant height of seedling 3-2) (Abe *et al.*, 2012).
486 *qPHS3-2* most likely corresponds to the gibberellin biosynthesis gene *GA20 oxidase1*
487 (*OsGA20ox1*), a paralog of *Semi Dwarf1* (*sd-1*, corresponding to *OsGA20ox2*) (Abe *et*
488 *al.*, 2012). Therefore, the pyramiding of *qPHS3-2* in NIL-*GF14h*^{Arroz} by marker-assisted
489 selection represents a promising approach for further improving seedling vigor in NIL-
490 *GF14h*^{Arroz}.

491 In recent years, "early-winter direct seeding" has been experimentally tested as a
492 new system of direct seeding for rice production in Japan (Shimono, 2020). In this system,
493 seeds are directly sown in the early winter of the previous year instead of the spring. The
494 sown seeds thus overwinter in snow-covered soil and germinate the following spring. The
495 major advantage of this approach is that it can significantly decrease the amount of labor
496 required by farmers during the busy spring season. However, it is challenging to

overwinter the seeds of modern rice varieties in the soil and achieve good seedling establishment (Shimono *et al.*, 2012; Oikawa *et al.*, 2019; Shimono, 2020). We expect that reintroducing beneficial alleles like *GF14h*^{Arroz} that were lost during modern breeding into future rice varieties will enable the implementation of new cultivation practices and increase productivity.

Acknowledgments

We thank the National Agriculture and Food Research Organization (NARO) gene bank, Japan, for providing rice seeds. This work was performed using the National Institute of Genetics (NIG) supercomputer at the Research Organization of Information and Systems (ROIS) National Institute of Genetics and the Academic Center for Computing and Media Studies (ACCMS) supercomputer at Kyoto University.

Competing interests

None declared.

Author contributions

AA, HT, and RT designed the research. YS, AA, KO, YS, HU, EK, KI, YO, TF, HT, MS, and HS performed experiments and analyzed the data. YS wrote the original manuscript. AA and RT edited the manuscript. All authors contributed to the manuscript and approved the submitted version.

References

Abe A, Takagi H, Fujibe T, Aya K, Kojima M, Sakakibara H, Uemura A, Matsuoka M, Terauchi R. 2012. OsGA20ox1, a candidate gene for a major QTL controlling seedling vigor in rice. *Theor Appl Genet* **125**(4): 647-657.

Ashikari M, Matsuoka M. 2006. Identification, isolation and pyramiding of quantitative trait loci for rice breeding. *Trends Plant Sci* **11**(7): 344-350.

525 **Bandelt HJ, Forster P, Rohl A. 1999.** Median-joining networks for inferring
526 intraspecific phylogenies. *Mol Biol Evol* **16**(1): 37-48.
527 **Bolger AM, Lohse M, Usadel B. 2014.** Trimmomatic: a flexible trimmer for Illumina
528 sequence data. *Bioinformatics* **30**(15): 2114-2120.
529 **Cabanettes F, Klopp C. 2018.** D-GENIES: dot plot large genomes in an interactive,
530 efficient and simple way. *PeerJ* **6**: e4958.
531 **Camoni L, Visconti S, Aducci P, Marra M. 2018.** 14-3-3 Proteins in Plant Hormone
532 Signaling: Doing Several Things at Once. *Front Plant Sci* **9**: 297.
533 **Cantu VA, Sadural J, Edwards R. 2019.** PRINSEQ++, a multi-threaded tool for fast
534 and efficient quality control and preprocessing of sequencing datasets. *PeerJ*
535 *Preprints* **7**: e27553v27551.
536 **Chen F, Li Q, Sun L, He Z. 2006.** The rice 14-3-3 gene family and its involvement in
537 responses to biotic and abiotic stress. *DNA Res* **13**(2): 53-63.
538 **Chen Y, Nie F, Xie SQ, Zheng YF, Dai Q, Bray T, Wang YX, Xing JF, Huang ZJ,**
539 **Wang DP, et al. 2021.** Efficient assembly of nanopore reads via highly accurate
540 and intact error correction. *Nat Commun* **12**(1): 60.
541 **De Coster W, D'Hert S, Schultz DT, Cruts M, Van Broeckhoven C. 2018.** NanoPack:
542 visualizing and processing long-read sequencing data. *Bioinformatics* **34**(15):
543 2666-2669.
544 **Fujino K, Obara M, Shimizu T, Koyanagi KO, Ikegaya T. 2015.** Genome-wide
545 association mapping focusing on a rice population derived from rice breeding
546 programs in a region. *Breed Sci* **65**(5): 403-410.
547 **Fujino K, Sekiguchi H, Matsuda Y, Sugimoto K, Ono K, Yano M. 2008.** Molecular
548 identification of a major quantitative trait locus, qLTG3-1, controlling low-

549 temperature germinability in rice. *Proc Natl Acad Sci U S A* **105**(34): 12623-
550 12628.
551 **Fujino K, Sekiguchi H, Sato T, Kiuchi H, Nonoue Y, Takeuchi Y, Ando T, Lin SY,**
552 **Yano M. 2004.** Mapping of quantitative trait loci controlling low-temperature
553 germinability in rice (Oryza sativa L.). *Theor Appl Genet* **108**(5): 794-799.
554 **Han LZ, Zhang YY, Qiao YL, Cao GL, Zhang SY, Kim JH, Koh HJ. 2006.** Genetic
555 and QTL analysis for low-temperature vigor of germination in rice. *Yi Chuan Xue*
556 *Bao* **33**(11): 998-1006.
557 **Hermeking H. 2003.** The 14-3-3 cancer connection. *Nat Rev Cancer* **3**(12): 931-943.
558 **Hori K, Sugimoto K, Nonoue Y, Ono N, Matsubara K, Yamanouchi U, Abe A,**
559 **Takeuchi Y, Yano M. 2010.** Detection of quantitative trait loci controlling pre-
560 harvest sprouting resistance by using backcrossed populations of japonica rice
561 cultivars. *Theor Appl Genet* **120**(8): 1547-1557.
562 **Itoh T, Onuki R, Tsuda M, Oshima M, Endo M, Sakai H, Tanaka T, Ohsawa R, Tabei**
563 **Y. 2020.** Foreign DNA detection by high-throughput sequencing to regulate
564 genome-edited agricultural products. *Sci Rep* **10**(1): 4914.
565 **Iwata N, Shinada H, Kiuchi H, Sato T, Fujino K. 2010.** Mapping of QTLs controlling
566 seedling establishment using a direct seeding method in rice. *Breeding Science*
567 **60**(4): 353-360.
568 **Jiang L, Liu S, Hou M, Tang J, Chen L, Zhai H, Wan J. 2006.** Analysis of QTLs for
569 seed low temperature germinability and anoxia germinability in rice (Oryza sativa
570 L.). *Field Crops Research* **98**(1): 68-75.
571 **Jiang N, Shi S, Shi H, Khanzada H, Wassan GM, Zhu C, Peng X, Yu Q, Chen X, He**
572 **X, et al. 2017.** Mapping QTL for Seed Germinability under Low Temperature

573 Using a New High-Density Genetic Map of Rice. *Front Plant Sci* **8**: 1223.

574 **Jiang S, Yang C, Xu Q, Wang L, Yang X, Song X, Wang J, Zhang X, Li B, Li H, et**
575 **al. 2020.** Genetic Dissection of Germinability under Low Temperature by
576 Building a Resequencing Linkage Map in japonica Rice. *Int J Mol Sci* **21**(4).

577 **Kim D, Paggi JM, Park C, Bennett C, Salzberg SL. 2019.** Graph-based genome
578 alignment and genotyping with HISAT2 and HISAT-genotype. *Nat Biotechnol*
579 **37**(8): 907-915.

580 **Kundu R, Casey J, Sung W-K. 2019.** HyPo: Super Fast & Accurate Polisher for Long
581 Read Genome Assemblies. *bioRxiv*: 2019.2012.2019.882506.

582 **Leigh JW, Bryant D, Nakagawa S. 2015.** popart: full-feature software for haplotype
583 network construction. *Methods in Ecology and Evolution* **6**(9): 1110-1116.

584 **Li H, Durbin R. 2009.** Fast and accurate short read alignment with Burrows-Wheeler
585 transform. *Bioinformatics* **25**(14): 1754-1760.

586 **Li H, Handsaker B, Wysoker A, Fennell T, Ruan J, Homer N, Marth G, Abecasis G,**
587 **Durbin R, Genome Project Data Processing S. 2009.** The Sequence
588 Alignment/Map format and SAMtools. *Bioinformatics* **25**(16): 2078-2079.

589 **Li L, Liu X, Xie K, Wang Y, Liu F, Lin Q, Wang W, Yang C, Lu B, Liu S, et al. 2013.**
590 qLTG-9, a stable quantitative trait locus for low-temperature germination in rice
591 (Oryza sativa L.). *Theor Appl Genet* **126**(9): 2313-2322.

592 **Madeira F, Tinti M, Murugesan G, Berrett E, Stafford M, Toth R, Cole C,**
593 **MacKintosh C, Barton GJ. 2015.** 14-3-3-Pred: improved methods to predict 14-
594 3-3-binding phosphopeptides. *Bioinformatics* **31**(14): 2276-2283.

595 **Mao F, Wu D, Lu F, Yi X, Gu Y, Liu B, Liu F, Tang T, Shi J, Zhao X, et al. 2022.** QTL
596 mapping and candidate gene analysis of low temperature germination in rice

597 (Oryza sativa L.) using a genome wide association study. *PeerJ* **10**: e13407.

598 **Mikami M, Toki S, Endo M. 2015.** Comparison of CRISPR/Cas9 expression constructs
599 for efficient targeted mutagenesis in rice. *Plant Mol Biol* **88**(6): 561-572.

600 **Miura K, Lin SY, Yano M, Nagamine T. 2001.** Mapping Quantitative Trait Loci
601 Controlling Low Temperature Germinability in Rice (Oryza sativa L.). *Breeding*
602 *Science* **51**(4): 293-299.

603 **Morrison DK. 2009.** The 14-3-3 proteins: integrators of diverse signaling cues that
604 impact cell fate and cancer development. *Trends Cell Biol* **19**(1): 16-23.

605 **Naito Y, Hino K, Bono H, Ui-Tei K. 2015.** CRISPRdirect: software for designing
606 CRISPR/Cas guide RNA with reduced off-target sites. *Bioinformatics* **31**(7):
607 1120-1123.

608 **Nguyen HN, Park I-K, Yeo S-M, Yun Y-T, Ahn S-N. 2012.** Mapping quantitative trait
609 loci controlling low-temperature germinability in rice. *Korean Journal of*
610 *Agricultural Science* **39**(4): 477-482.

611 **Oikawa S, Nishi M, Yui S, Kashiwagi J, Nakashima T, Ichikawa S, Kimura T,**
612 **Ohdaira Y, Nagasuga K, Kuroda E, et al. 2019.** Improvement of Seedling
613 Establishment by Seed Coating with Iron in Early-winter Direct-sowing Rice.
614 *Japanese Journal of Crop Science* **88**(4): 259-267.

615 **Okuno K. 2004.** Molecular Mechanisms of Cold Tolerance in Rice and Wheat. *Thermal*
616 *Medicine(Japanese Journal of Hyperthermic Oncology)* **20**(2): 51-60.

617 **Pan Y, Zhang H, Zhang D, Li J, Xiong H, Yu J, Li J, Rashid MA, Li G, Ma X, et al.**
618 **2015.** Genetic analysis of cold tolerance at the germination and booting stages in
619 rice by association mapping. *PLoS One* **10**(3): e0120590.

620 **Pan Z, Tan B, Cao G, Zheng R, Liu M, Zeng R, Wang S, Zhu H, Ye H, Zhao G, et al.**

621 **2021.** Integrative QTL Identification, Fine Mapping and Candidate Gene Analysis
622 of a Major Locus qLTG3a for Seed Low-Temperature Germinability in Rice. *Rice*
623 *(N Y)* **14**(1): 103.
624 **Pertea M, Pertea GM, Antonescu CM, Chang TC, Mendell JT, Salzberg SL. 2015.**
625 StringTie enables improved reconstruction of a transcriptome from RNA-seq
626 reads. *Nat Biotechnol* **33**(3): 290-295.
627 **Roach MJ, Schmidt SA, Borneman AR. 2018.** Purge Haplotigs: allelic contig
628 reassignment for third-gen diploid genome assemblies. *BMC Bioinformatics*
629 **19**(1): 460.
630 **Satoh T, Tezuka K, Kawamoto T, Matsumoto S, Satoh-Nagasawa N, Ueda K,**
631 **Sakurai K, Watanabe A, Takahashi H, Akagi H. 2015.** Identification of QTLs
632 controlling low-temperature germination of the East European rice (Oryza sativa
633 L.) variety Maratteli. *Euphytica* **207**(2): 245-254.
634 **Shakiba E, Edwards JD, Jodari F, Duke SE, Baldo AM, Korniliev P, McCouch SR,**
635 **Eizenga GC. 2017.** Genetic architecture of cold tolerance in rice (Oryza sativa)
636 determined through high resolution genome-wide analysis. *PLoS One* **12**(3):
637 e0172133.
638 **Shim KC, Kim SH, Lee HS, Adeva C, Jeon YA, Luong NH, Kim WJ, Akhtamov M,**
639 **Park YJ, Ahn SN. 2020.** Characterization of a New qLTG3-1 Allele for Low-
640 temperature Germinability in Rice from the Wild Species Oryza rufipogon. *Rice*
641 *(N Y)* **13**(1): 10.
642 **Shimono H. 2020.** New technique : Early- winter direct- sowing cultivation in rice under
643 cool climate. *Regulation of Plant Growth & Development* **55**(1): 63-66.
644 **Shimono H, Abe A, Kim CH, Sato C, Iwata H. 2023.** Upcycling rice yield trial data

using a weather-driven crop growth model. *Commun Biol* **6**(1): 764.

Shimono H, Tamai M, Hamasaki T, Sagawa R, Ohtani R. 2012. Effects of Autumn Direct-seeding on Rice Growth and Yield under Cool Climates. *Japanese Journal of Crop Science* **81**(1): 93-98.

Sugihara Y, Abe Y, Takagi H, Abe A, Shimizu M, Ito K, Kanzaki E, Oikawa K, Kourelis J, Langner T, et al. 2023. Disentangling the complex gene interaction networks between rice and the blast fungus identifies a new pathogen effector. *PLoS Biol* **21**(1): e3001945.

Sugihara Y, Young L, Yaegashi H, Natsume S, Shea DJ, Takagi H, Booker H, Innan H, Terauchi R, Abe A. 2022. High-performance pipeline for MutMap and QTL-seq. *PeerJ* **10**: e13170.

Sun J, Zhang G, Cui Z, Kong X, Yu X, Gui R, Han Y, Li Z, Lang H, Hua Y, et al. 2022. Regain flood adaptation in rice through a 14-3-3 protein OsGF14h. *Nat Commun* **13**(1): 5664.

Takagi H, Abe A, Yoshida K, Kosugi S, Natsume S, Mitsuoka C, Uemura A, Utsushi H, Tamiru M, Takuno S, et al. 2013. QTL-seq: rapid mapping of quantitative trait loci in rice by whole genome resequencing of DNA from two bulked populations. *Plant J* **74**(1): 174-183.

Tanaka N, Shenton M, Kawahara Y, Kumagai M, Sakai H, Kanamori H, Yonemaru J, Fukuoka S, Sugimoto K, Ishimoto M, et al. 2020. Whole-Genome Sequencing of the NARO World Rice Core Collection (WRC) as the Basis for Diversity and Association Studies. *Plant Cell Physiol* **61**(5): 922-932.

Tanaka N, Shenton M, Kawahara Y, Kumagai M, Sakai H, Kanamori H, Yonemaru JI, Fukuoka S, Sugimoto K, Ishimoto M, et al. 2021. Investigation of the

669 Genetic Diversity of a Rice Core Collection of Japanese Landraces using Whole-
670 Genome Sequencing. *Plant Cell Physiol* **61**(12): 2087-2096.
671 **Toki S, Hara N, Ono K, Onodera H, Tagiri A, Oka S, Tanaka H. 2006.** Early infection
672 of scutellum tissue with Agrobacterium allows high-speed transformation of rice.
673 *Plant J* **47**(6): 969-976.
674 **Vaser R, Sovic I, Nagarajan N, Sikic M. 2017.** Fast and accurate de novo genome
675 assembly from long uncorrected reads. *Genome Res* **27**(5): 737-746.
676 **Wang X, Zou B, Shao Q, Cui Y, Lu S, Zhang Y, Huang Q, Huang J, Hua J. 2018.**
677 Natural variation reveals that OsSAP16 controls low-temperature germination in
678 rice. *J Exp Bot* **69**(3): 413-421.
679 **Wilson RS, Swatek KN, Thelen JJ. 2016.** Regulation of the Regulators: Post-
680 Translational Modifications, Subcellular, and Spatiotemporal Distribution of
681 Plant 14-3-3 Proteins. *Front Plant Sci* **7**: 611.
682 **Yabe S, Yoshida H, Kajiya-Kanegae H, Yamasaki M, Iwata H, Ebana K, Hayashi T,**
683 **Nakagawa H. 2018.** Description of grain weight distribution leading to genomic
684 selection for grain-filling characteristics in rice. *PLoS One* **13**(11): e0207627.
685 **Yang T, Zhou L, Zhao J, Dong J, Liu Q, Fu H, Mao X, Yang W, Ma Y, Chen L, et al.**
686 **2020.** The Candidate Genes Underlying a Stably Expressed QTL for Low
687 Temperature Germinability in Rice (Oryza sativa L.). *Rice (N Y)* **13**(1): 74.
688 **Yoshida H, Hirano K, Yano K, Wang F, Mori M, Kawamura M, Koketsu E, Hattori**
689 **M, Ordonio RL, Huang P, et al. 2022.** Genome-wide association study identifies
690 a gene responsible for temperature-dependent rice germination. *Nat Commun*
691 **13**(1): 5665.
692 **Zhang B, Ma L, Wu B, Xing Y, Qiu X. 2022.** Introgression Lines: Valuable Resources

693 for Functional Genomics Research and Breeding in Rice (Oryza sativa L.). *Front*
694 *Plant Sci* **13**: 863789.
695 **Zhao Q, Feng Q, Lu H, Li Y, Wang A, Tian Q, Zhan Q, Lu Y, Zhang L, Huang T, et**
696 **al. 2018.** Pan-genome analysis highlights the extent of genomic variation in
697 cultivated and wild rice. *Nat Genet* **50**(2): 278-284.
698
699

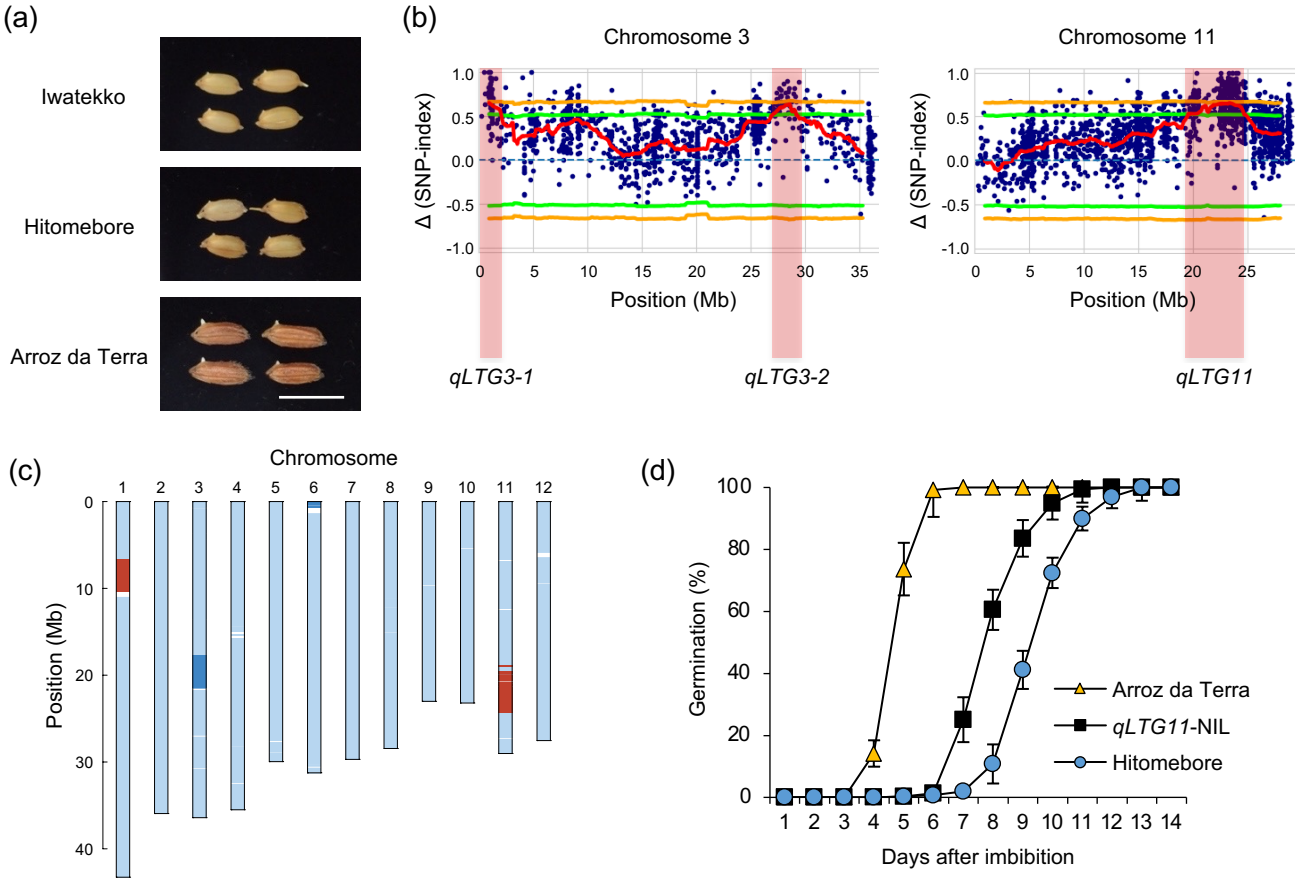

Fig 1. Effects of quantitative trait loci (QTLs) on low-temperature seed germinability.
(a) Representative photographs showing the germination of seeds from the Iwatekko, Hitomebore, and Arroz da Terra varieties 10 days after the onset of seed imbibition at 15° C. Scale bar, 1 cm. **(b)** Map positions of QTLs for low-temperature germination, as determined by QTL-seq. The Δ (SNP-index) values (red lines) were plotted for chromosomes 3 and 11, with statistical confidence intervals under the null hypothesis of no QTL (green, $P < 0.05$; orange, $P < 0.01$). **(c)** Diagram showing the genotype of *qLTG11*-NIL. *qLTG11*-NIL harbors the Arroz da Terra allele at *qLTG11* on chromosome 11. Light blue indicates genomic fragments from Hitomebore; red indicates genomic fragments from Arroz da Terra; dark blue indicates heterozygous regions. **(d)** Germination time courses of Hitomebore, *qLTG11*-NIL, and Arroz da Terra at 15° C. Values are means ± standard deviation (SD) from biologically independent samples (Hitomebore and NIL, $n = 10$; Arroz da Terra, $n = 5$).

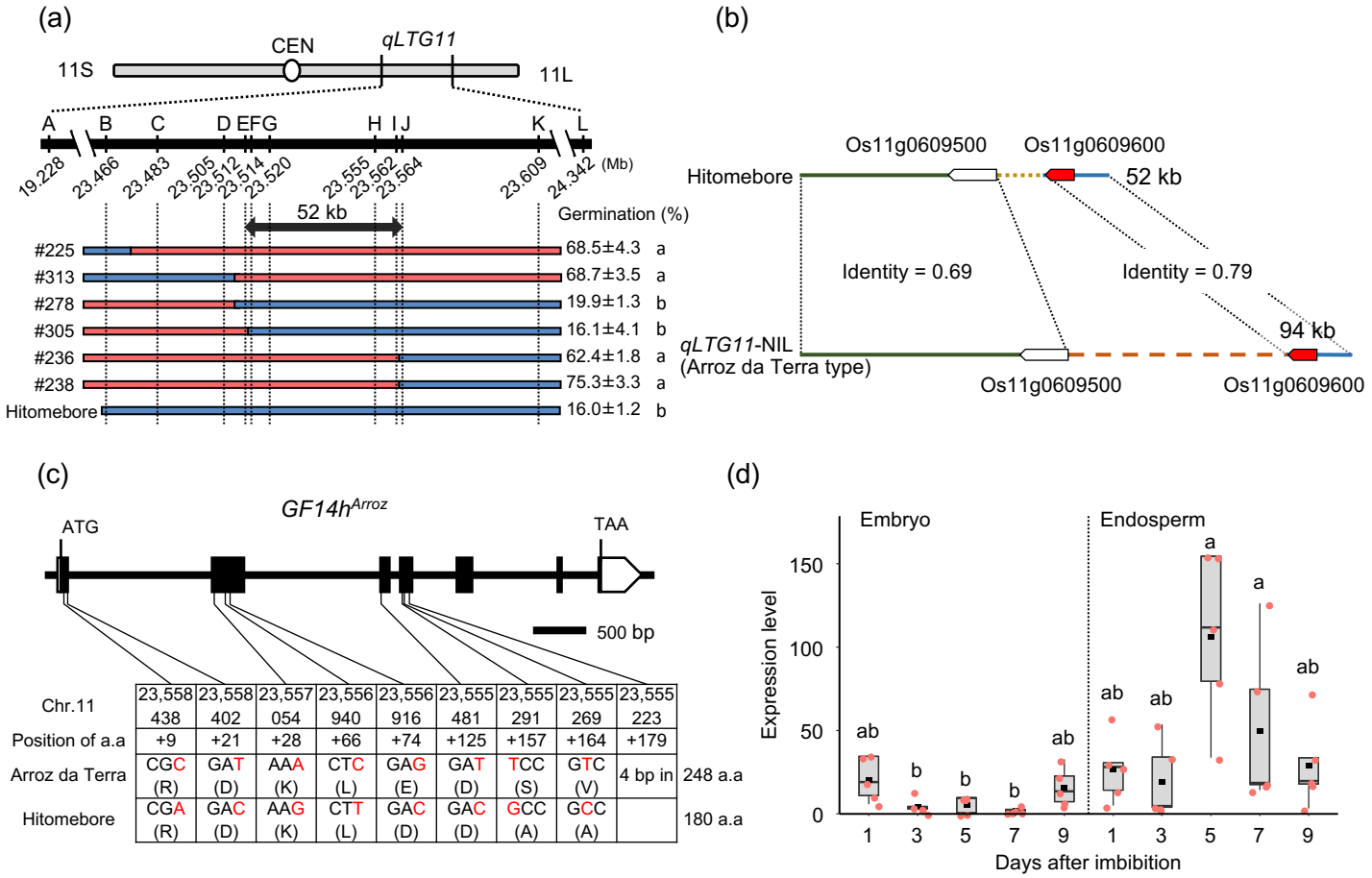

Fig 2. Positional cloning of *qLTG11*.

(a) Fine mapping of *qLTG11* to a 52-kb region between markers E and J. The chromosomal positions are based on the Nipponbare reference genome (Os-Nipponbare-Reference-IRGSP-1.0). Germination percentage was determined at 9 days of incubation at 15° C. Red and blue rectangles indicate chromosomal segments homozygous for Arroz da Terra or Hitomebore, respectively. Different lowercase letters indicate significant differences (n = 3 biologically independent samples, $P < 0.001$, Tukey's HSD test). **(b)** Genomic structure of the candidate genomic region in Arroz da Terra and Hitomebore. Os11g0609600 (shown in red), encoding GF14h, is expressed in germinating seeds. **(c)** Diagram of the *GF14h* gene structure and sequence polymorphisms between Arroz da Terra and Hitomebore. The chromosomal positions are based on the Nipponbare reference genome. The coding region of *GF14h* in Hitomebore is identical to that in Nipponbare. The 4-bp deletion in Hitomebore causes a frameshift and the introduction of a premature stop codon. **(d)** Relative *GF14h* expression levels in germinating seeds of *qLTG11*-NIL. In the boxplots, the box edges represent the upper and lower quantiles, the horizontal line in the middle of the box represents the median value, whiskers represent the lowest quantile to the top quantile, and the black squares show the mean. Five biological replicates were measured independently. Different lowercase letters indicate significant differences based on Tukey's HSD test ($P < 0.05$). *OsActin1* (Os03g0718100) was used for normalization.

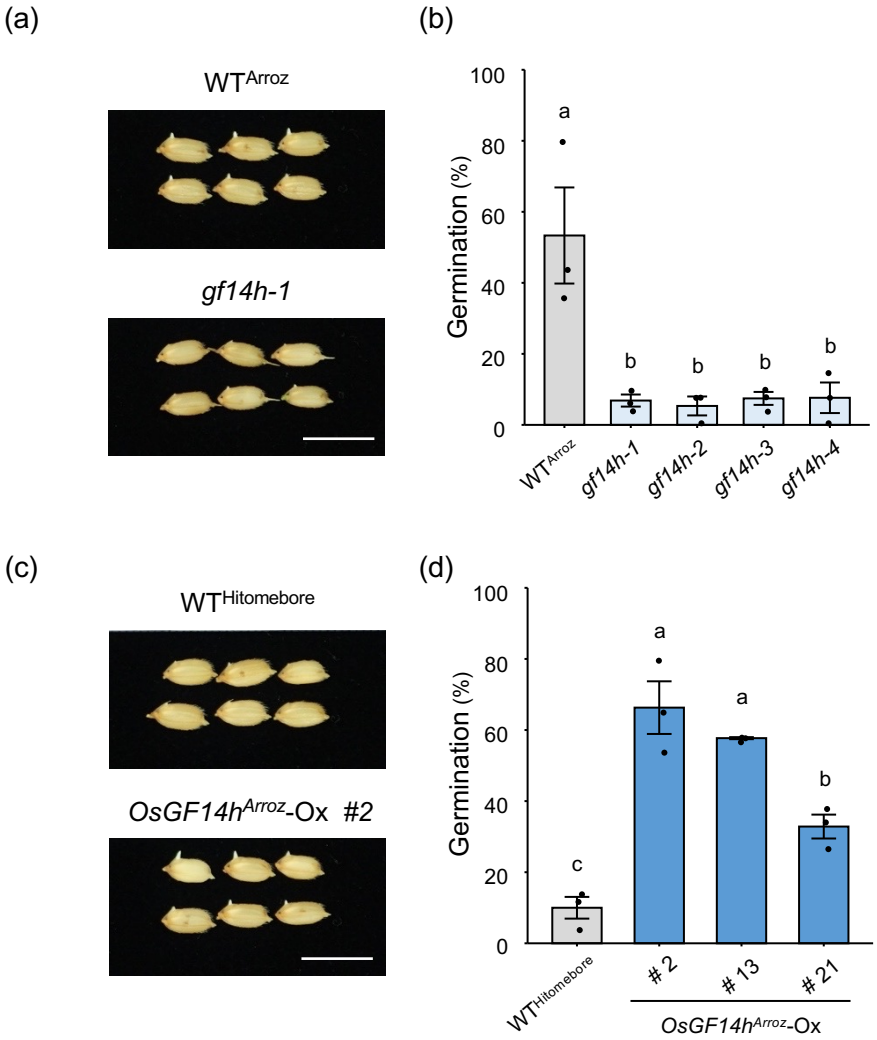

Fig 3. Effect of *GF14h* mutation and overexpression on low-temperature germination. **(a)** Representative photographs showing seed germination in wild-type harboring Arroz-type *GF14h* (WT^{Arroz}) and CRISPR/Cas9 knockout lines (*gf14-1*) at 8 days after the onset of seed imbibition. Scale bar, 1 cm. **(b)** Seed germination rate of WT^{Arroz} and its CRISPR/Cas9 knockout lines at 7 days of seed imbibition at 15° C. The two target constructs (Fig. S8) were introduced into the *qLTG11*-NIL line. Data are means ± standard error (SE, n = 3). Different lowercase letters indicate significant differences based on Tukey's HSD test (P < 0.01). **(c)** Representative photographs showing seed germination of wild-type ($WT^{Hitomebore}$) and $OsGF14h^{Arroz}$ overexpression lines ($OsGF14h^{Arroz}$-Ox #2) at 7 days of seed imbibition at 15ºC. Scale bar, 1 cm. **(d)** Seed germination rate of $WT^{Hitomebore}$ and $GF14h^{Arroz}$ overexpression lines in the Hitomebore background at 7 days of seed imbibition at 15° C. Data are means ± SE (n = 3). Different lowercase letters indicate significant differences based on Tukey's HSD test (P < 0.05).

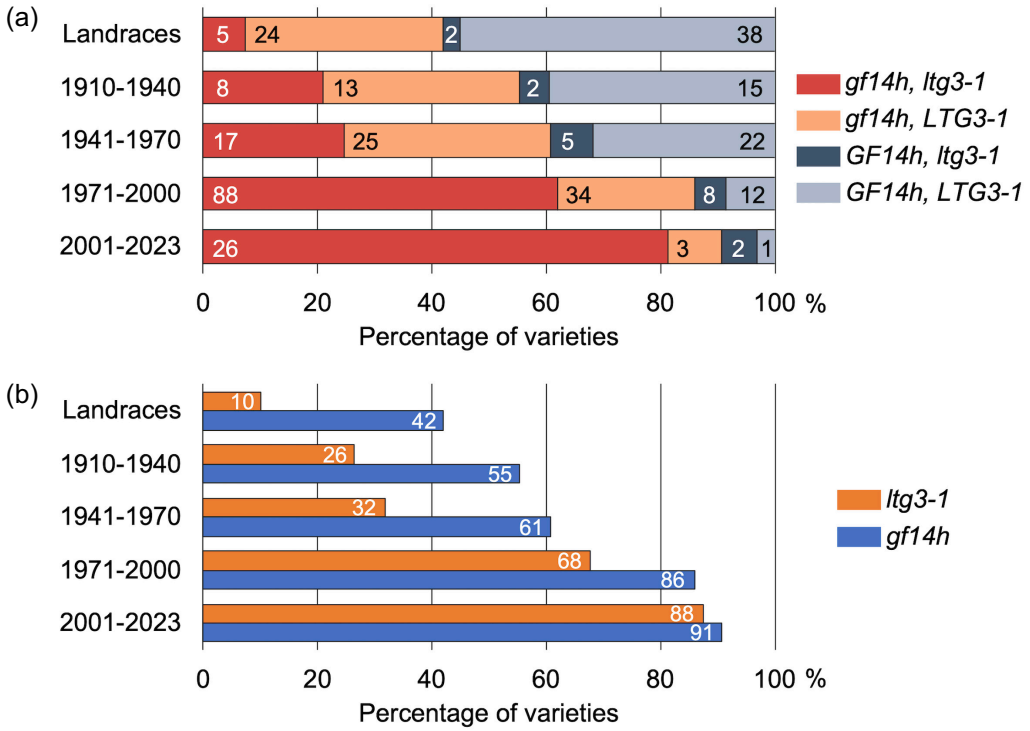

Fig 4. Gradual selection of loss-of-function alleles in *GF14h* and *qLTG3-1* during rice breeding in Japan.

A total of 350 Japanese varieties were examined, including the World Rice Core Collection (Tanaka *et al*., 2020), the Rice Core Collection of Japanese Landraces (Tanaka *et al*., 2021), and the collection of Japanese core cultivars (Shimono *et al*., 2023). The allele type at each gene was determined to be functional or nonfunctional by the k-mer method using Illumina short reads for each variety. **(a)** Proportion of allele type combinations at *GF14h* and *qLTG3-1* sorted by breeding year. **(b)** Proportion of nonfunctional allele types at *GF14h* and *qLTG3-1* sorted by breeding year.

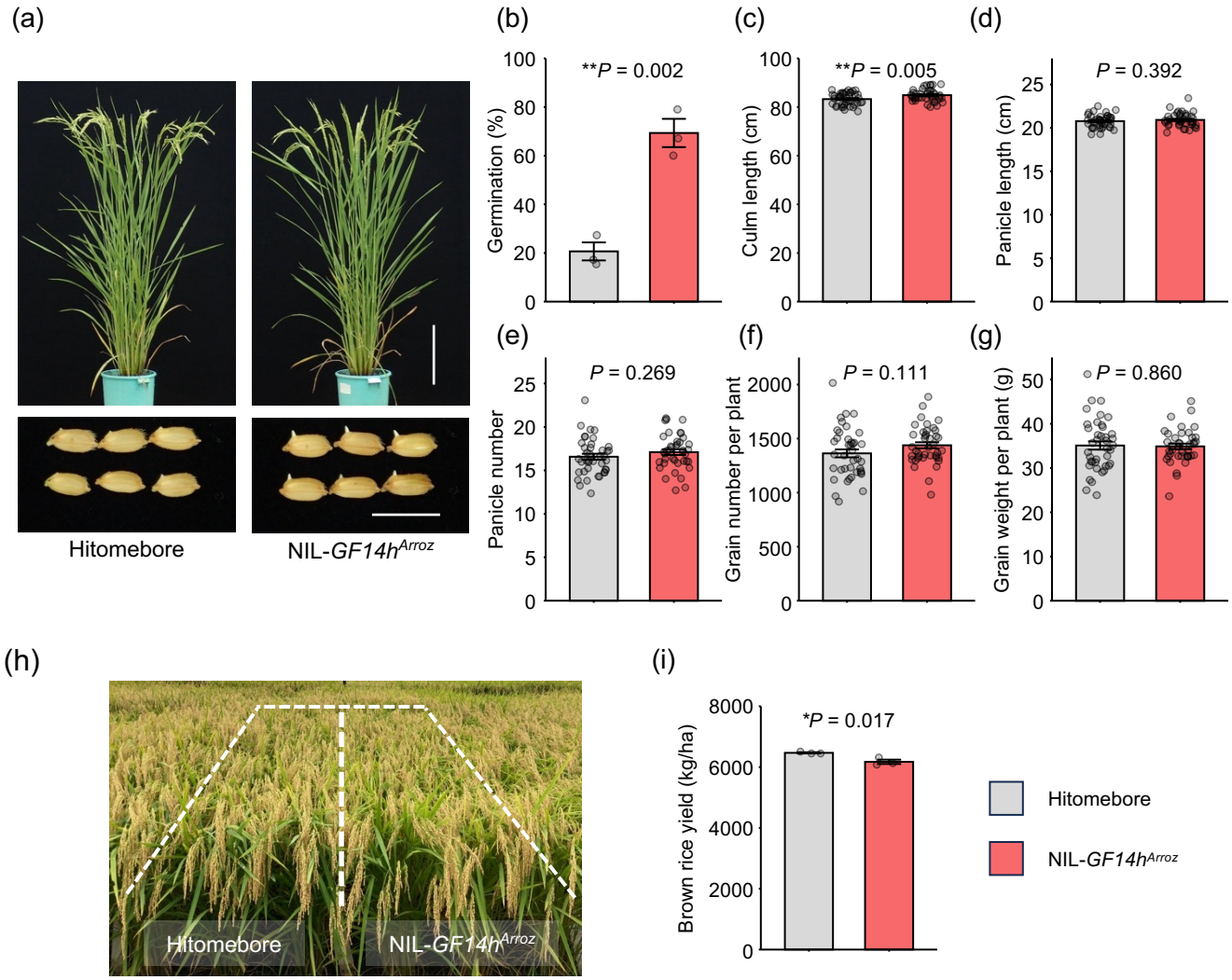

Fig 5. Phenotypic analysis of a near-isogenic line homozygous for Arroz-type *GF14h* in the Hitomebore genetic background (NIL-*GF14h*^{Arroz}).

(a) Gross morphology of Hitomebore and NIL-*GF14h*^{Arroz} at 87 days after transplanting (top row), and seed germination at 9 days after the onset of seed imbibition at 15° C (bottom row). Scale bars, 20 cm (top), 1 cm (bottom). **(b)** Low-temperature germination ability of NIL-*GF14h*^{Arroz} at 8 days after the onset of seed imbibition at 15° C. Values are means ± SE of biologically independent samples (n = 3). Asterisks indicate significant differences, as determined by two-tailed t-test. **(c–g)** Agronomic traits in Hitomebore and NIL-*GF14h*^{Arroz}: culm length (**c**), panicle length (**d**), panicle number (**e**), grain number per plant (**f**), and grain weight per plant (**g**). Values are means ± SE of biologically independent plants (n = 40). **(h)** Side view of Hitomebore and NIL-*GF14h*^{Arroz} growing in the field under typical rice-growing conditions at the maturity stage. **(i)** Brown rice yield per unit area. Values are means ± SE of biologically independent plots (n = 3). P-values calculated by t-tests are listed throughout the figure.